Int. J. Nanosci. Nanotechnol., Vol. 16, No. 2, June 2020, pp. 117-125

Amido-Amino Clay Stabilized Copper Nanoparticles: Antimicrobial Activity and Catalytic Efficacy for Aromatic Amination

Ananya Shibana T[1], Jaculin Raiza[2] and Kannaiyan Pandian[2,*]

[1]Department of Chemistry, Pondicherry University, Pondicherry, PY 605014 India.
[2]Department of Inorganic Chemistry, University of Madras, Guindy Campus, Chennai, TN 600025 India.

(*) Corresponding author: jeevapandian@yahoo.co.uk
(Received: 09 November 2019 and Accepted: 15 January 2020)

Abstract

Amido-amino functionalized halloysite stabilized copper nanoparticles (aah-CuNPs) were synthesized through one-pot protocol by a wet chemical method using hydrazine as reducing agent. The nanocomposite formed was stable in dry ethanol. The composition and binding nature of the nanocomposite were studied using FT-IR, DRS-UV, EDAX and powder XRD techniques. The morphological features of the composite were obtained from HRSEM analysis. The thermal stability of the copper nanocomposites was studied using TGA analysis. The prepared nanocomposite displayed broad spectrum antimicrobial activity, and it was very effective in Ullmann aromatic amination reaction.

Keywords: *Amido-amino clay, Aromatic amination, Catalysis, Copper nanoparticles, Ullmann reaction.*

1. INRODUCTION

Construction of aryl-N and aryl-O bonds through cross-coupling reactions is one of the useful methods for the synthesis of various bioactive aryl compounds. Metal catalysts, in particular, copper plays a key role in the cross-coupling reactions of activated as well as inactivated aromatic halides [1-9]. Other metal catalysts such as cobalt, indium, nickel, bismuth, silver, gold and iron have also been explored for such aromatic nucleophilic substitution reactions [10, 11].

One of the earliest examples of metal-mediated arylation of amines in the presence of a copper salt, was reported by Ullman in 1903 [12]. Later, palladium catalyst based amination reactions were developed that did not suffer from issues such as low yield and stoichiometric amount of catalyst as associated with Ullman reaction [13]. The relatively higher cost of palladium eventually motivated a renewed interest in copper catalyzed amination methods that are complementary to those of palladium based catalytic reactions. Despite the uncertainty regarding the mechanism of copper based catalytic reactions single-electron transfer and oxidative addition/reductive elimination pathways), copper-catalyzed amination has been applied in a number of syntheses of natural products. Aromatic or heteroaromatic halides are the most common electrophiles employed.

The Ullmann-type reactions based on copper-catalyzed nucleophilic aromatic substitution between various nucleophiles and aryl halides is well known in organic synthesis. Recently, ligand-free copper-catalyzed arylation of amidines [14], copper-catalyzed synthesis of 4-amino-quinazoline and 2,4-diaminoquinazoline derivatives [15], copper-catalyzed amination of bromobenzoic acids using aliphatic and aromatic amines [16], copper-catalyzed coupling of alkylamines and aryl iodides even in air atmosphere [17], copper powder-catalyzed organic solvent- and

ligand-free Ullmann amination of aryl halides [18], CuI/DMPAO-catalyzed N-arylation of acyclic secondary amines [19], CuI/oxalic diamide catalyzed coupling reaction of (hetero)aryl chlorides and amines [20], copper oxide-catalyzed aryl amination [21] and copper-catalyzed cross-coupling reactions of aryl iodides with amides, thiols, and phenols [22] have been reported.

In this report, we present the application of amido - amino halloysite stabilized copper nanoparticles. We provide evidence for the antimicrobial property of the synthesized nanoparticles, which would be useful in the fabrication of drinking water filters. It is inferred that the amido-amino halloysite best stabilizes copper nanoparticles and avoids the oxidation of copper nanoparticles into copper oxide nanocomposites. We wanted to explore the advantage of this solid-supported catalyst for reusability and antimicrobial activity. We have explored a new methodology to exploit the use of substituted benzylamines in Ullmann amination. An application of this nanocomposite catalyst in Ullmann amination of 2,6-dibromopyridine in DMSO medium is demonstrated. The catalyst could be reused for three cycles without significant loss in its activity. The protocol was simple and efficient, avoiding the need for inert atmosphere, additional base or other additives.

2. MATERIALS AND METHODS

2.1. Chemicals and Solvents

Ethanol (>99.9%) was purchased from Merck. All solutions were prepared in Milli Q water and all apparatus were washed with double distilled water. Amido-amino halloysite was synthesized in the lab using a previously reported method [23]. Hydrazine hydrate, methoxy benzylamine derivatives and 2,6-dibromopyridine were purchased from Sigma-Aldrich, Bangalore. All reagents and solvents used in this study were of reagent grade.

2.2 Instrumental Analysis

Fourier-transform infrared spectra were recorded on Thermo Scientific Inc., NICOLET iS10 FT-IR Spectrometer. ^{1}H and ^{13}C NMR were recorded on Brüker Advance 400 MHz, in CDCl3 using tetramethylsilane as the internal standard. Chemical shifts were reported in parts per million (ppm) downfield with reference to tetramethylsilane. HRSEM images were recorded on FEIQUANTA 200 SEM, Environmental SEM. The Energy Dispersive x-ray spectrum was recorded on EDX Oxford Instrument. TGA analysis was carried out on Thermogravimetric Analyser, V4.4A: TA Instruments, USA. DRS-UV spectrum was recorded on Shimadzu UV-2600, Japan.

2.3 Synthesis of Amido-Amino Clay Stabilized Copper Nanoparticles (aah-CuNPs)

Amido-amino halloysite was synthesized using a procedure optimized in the lab [23, 24]. The amido-amino halloysite was first exfoliated by dispersing 200 mg of clay in 10 mL Milli Q water by sonication for 2 minutes. Copper precursor (10.0 mL of 10 mM $CuSO_4$ solution) was added followed by the drop wise addition of hydrazine hydrate (10.0 mL of 1M solution of hydrazine hydrate) and continuous stirring using a magnetic stirrer. The color of the solution changed from blue to dark red, indicating the reduction of Cu^{2+} to Cu^{0} and the formation of nanoparticles. The solution was stirred for 10 minutes after the addition of hydrazine hydrate was complete. Then, a known amount of amido-amino halloysite was added to the reaction mixture and stirring was continued for 30 minutes. After workup and precipitation in ethanol, the amido-amino halloysite stabilized copper nanoparticles were stored in ethanol at 5 ^{o}C until they were used for the reaction.

2.4 Antimicrobial Assay

The antimicrobial activity of the synthesized aah-CuNPs was studied using fresh

subcultures obtained from overnight grown cultures of *Escherichia coli, Staphylococcus aureus, Salmonella typhimurium, Klebsiella pneumonia, Bacillus cereus, Proteus vulgaris, Pseudomonas aeruginosa* and *Candida albicans*. The aah-CuNps were tested for their antimicrobial activities in vitro using the agar diffusion technique.

Antibacterial of extracts was determined by disc diffusion method on Muller Hinton agar (MHA) medium. Muller Hinton Agar (MHA) medium is poured in to the petri plate. After the medium was solidified, the inoculums were spread on the solid plates with sterile swab moistened with the bacterial suspension. The disc were placed in MHA plates and add 20 µL of sample (Concentration: 1000µg, 750 µg and 500 µg) were placed in the disc. The plates were incubated at 37ºC for 24 hrs. Then the antimicrobial activity was determined by measuring the diameter of zone of inhibition [23].

Antifungal activity of the sample was determined by disc diffusion method on Sabouraud Dextrose Agar (SDA) medium. SDA medium was poured in to the petri plate. After the medium was solidified, the inoculums were spread on the agar plates with sterile swab soaked with the fungal suspension. Amphotericin-B was taken as positive control. Samples and positive control of 20 µL each were added in sterile discs and placed in SDA plates. The plates were incubated at 28ºC for 24 hrs. Then antifungal activity was determined by measuring the diameter of zone of inhibition.

2.5 Synthesis of 6 – bromo – N - (4 - methoxybenzyl) Pyridin – 2 - amine Catalyzed by aah-CuNPs

2,6-Dibromopyridine (0. 2g, 0.84 mmol) and 3,4-dimethoxybenzlamine (1.0 mL, 6.8 mmol) were mixed in dimethylsulfoxide (2.5 mL), and the mixture was stirred at 100-110°C in an oil bath for 4 hours. This reaction was catalyzed by aah-CuNPs (~20.0 mg). After completion of the reaction (as monitored through TLC), the mixture was poured into water, and the aqueous solution was extracted with DCM (3×20 mL). Workup with brine, and evaporation of DCM yielded a colorless solid that did not require further purification.

3. RESULTS AND DISCUSSION

Amido-amino clay stabilized copper nanoparticles were synthesized by slight modification of the procedure described previously [24, 25]. The synthesized aah-CuNPs were characterized using HR SEM, FT-IR, DRS UV and EDAX techniques and the thermal stability was studied using TGA analysis.

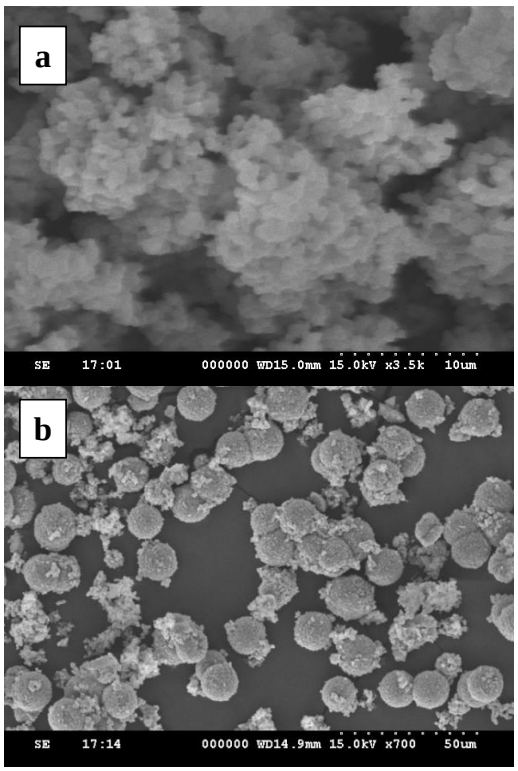

Figure 1. *(a) The SEM image of the CuNPs doped with amido-amino halloysite; (b) Closer-view of SEM image of aah-CuNps.*

3.1 Morphology

As seen in Figure 1, the aah-CuNPs show spherical shape and uniform size. The particle size distribution seen in Figure 1a reveals that the amido-amino halloysite

particles are agglomerated with a coarse morphology, and the size of clay particles is small enough to stabilize the larger CuNPs. For clarity and comparative account, HR SEM images of amido-amino clay and aah-CuNPs are also provided in Figure 1. The fact that all the nanoparticles are well separated, and no clusters or aggregated mass is seen, clearly indicates the stabilization of individual aah-CuNPs by the interaction of amido-amino clay with CuNPs.

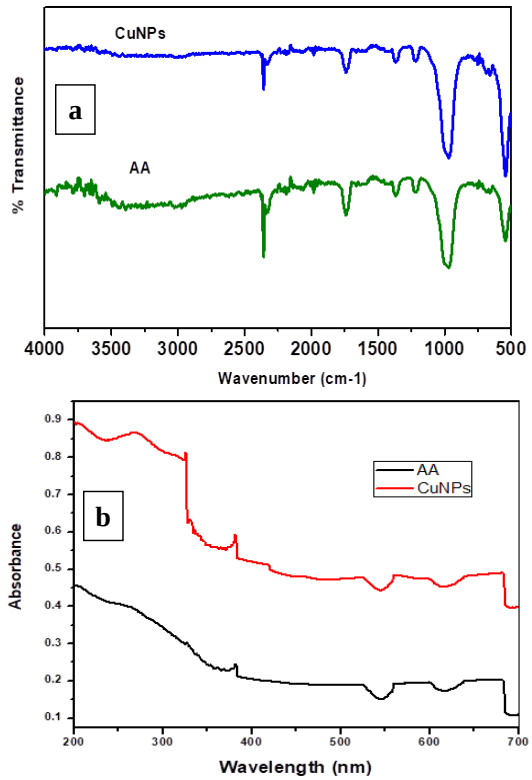

Figure 2. *FT-IR (a) and DRS-UV (b) spectra of amido-amino halloysite (AA; lower trace) and clay stabilized by CuNPs (aah-CuNPs; upper trace).*

3.2 Spectroscopic Characterization

The FT-IR spectrum of amido-amino halloysite (Figure 2a) displays three characteristic absorptions at ~1750, 1000 and 560 cm^{-1}. The band at ~1730 nm is assigned to different deformation modes of the amido-amino propyl groups: N-H bending and C=O stretching) [24,25]. The strong band at ~1000 cm^{-1} is attributed to Si-O-Si asymmetric stretching mode. The band ~560 cm^{-1} could be due to the bending of Al-O-Si and Si-O-Si in the octahedral layer of the amido-amino halloysite composite [26]. The weak band at 1381 cm^{-1} is due to the formation of the amine carbamate linkage [24,25]. Comparison of FT-IR and DRS UV spectra of amido-amino clay, with and without CuNPs (Figure 2), reveals the presence of amido-amino halloysite particles in all the samples, indicating the interaction of amido-amino halloysite with CuNPs and stabilization of aah-CuNPs in the powder form as well.

3.3 EDX Report and Thermal Stability

The percentage of copper present in aah-CuNPs was studied by Energy Dispersive X-ray (EDX) spectroscopy. Figure 3a confirms the presence of CuNps and other elements from amido-amino halloysite. From a comparison of the different peaks in the spectrum, it could be concluded that the individual nanoparticles consisting of copper showed weak signals, and the groups of copper nanoparticles showed strong signals in the EDX spectrum.

The powder XRD pattern of aah-CuNPs is shown in Figure 3b. The absence of 10Å peak clearly indicates that halloysite is dehydrated in aah-CuNPs powder. Further, the reflections expected from dehydrated halloysite are observed as shown in Figure 3b, which indicate the formation of aah-CuNPs [27].

The thermal stability of amido-amino halloysite before and after incorporation of CuNPs was determined by thermogravimetric analysis (TGA). The TGA thermograms of clay and clay-stabilized copper nanoparticles are shown in Figure 3b. The thermogram of amido-amino halloysite shows steady weight loss (up to 20%) due to the removal of chemisorbed water molecules and moisture as the temperature is increased from 10 to 250 °C. The weight loss remains negligible above 250 °C and up to 800 °C. This observation confirms the stability of amido-amino halloysite at higher temperatures. However, amido-amino

halloysite stabilized CuNPs are stable up to 180 °C, and about 58% weight loss is observed between 180 and 280 °C. This major weight loss is ascribed to the degradation of linkage between CuNPs and amido-amine halloysite.

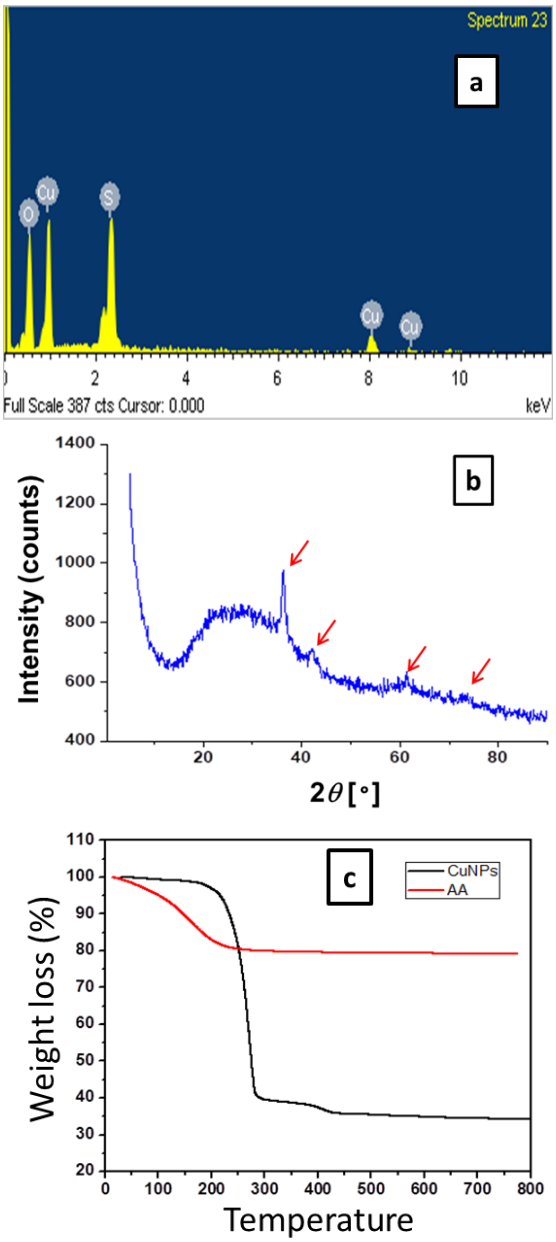

Figure 3. *The EDX spectrum of monodispersed amido-amino halloysite clay-stabilized CuNPs (a), Powder XRD spectrum of aah-CuNPs (b) and TGA curves (c) of amido-amino halloysite clay (red line) and aah-CuNPs (dark line) showing their thermal stability.*

The second step of degradation due to propylamido-amine group was observed between 390 and 420 °C with a weight loss of about 5%. The weight loss above 420 °C was negligible. For practical purposes, amido-amino halloysite stabilized CuNPs exhibit improved thermal stability as compared with amido-amino halloysite.

3.4 Antimicrobial Activity of Amido-Amino Clay Stabilized CuNPs

The development of nanocomposites with antimicrobial activity offers interesting nanostructures with size and shape dependent properties that can be exploited [28,29]. The introduction of copper nanoparticles onto porous material like amido-amino halloysite might be useful to avoid bacterial contamination in the fabrication of drinking water filters. Therefore, we explored the antimicrobial activity of aah-CuNPs. The procedure was performed using cup plate method as recommended in Indian Pharmacopoeia (Anonymous 1996).

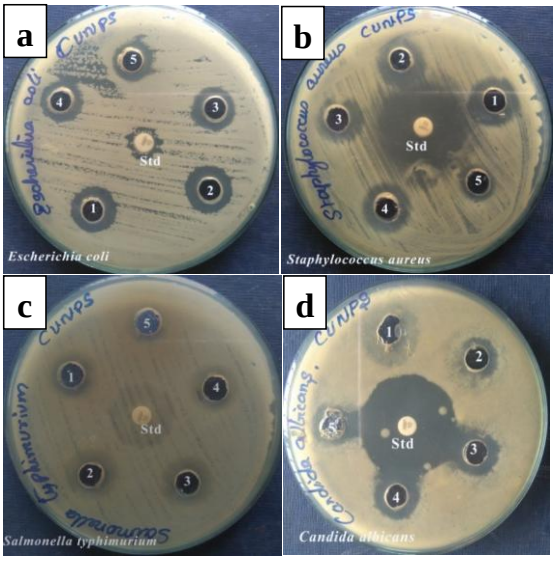

Figure 4. *Agar plate assay indicating the zone of inhibiton by aah-CuNPs at the different concentration against (a) E. coli, (b) S. aureus, (c) S. typhimurium and (d) C. albicans.*

The observed antimicrobial activity of aah-CuNPs against *Escherichia coli,*

Staphylococcus aureus, Salmonella typhimurium, Klebsiella pneumonia, Bacillus cereus, Proteus vulgaris, Pseudomonas aeruginosa and Candida albicans are collected in Table 1. In all the cases, the zone of inhibition appears to decrease when the amount of aah-CuNPs is decreased due to dilution [30]. The zone of inhibition at the highest concentration used for the present study varied from 9 mm to 19 mm, indicating the microbial species specific activity of aah-CuNPs. Presence of clean zones of inhibition clearly indicates the disruption of cells and suggests that aah-CuNPs have biocidal property.

Table 1. *Nanoparticle induced zone of inhibition of microbial growth in agar medium. Well diameter was 6 mm. Solvent used was DMSO-water (1:1) mixture.*

Microbial organism	Zone of inhibition (mm) versus Amount of nanoparticles (mg/mL)								
	5	2.5	1.25	0.62	0.31	0.15	0.07	0.03	Std
E. coli	19	18	15	12	11	10	9	-	-VE
S. aureus	19	17	15	13	10	-	-	-	+VE
S. typhimurium	17	14	13	12	9	-	-	-	-VE
K. pneumoniae	-	-	-	-	-	-	-	-	-VE
B. cereus	-	-	-	-	-	-	-	-	-VE
P. vulgaris	-	-	-	-	-	-	-	-	-VE
P. aeruginosa	-	-	-	-	-	-	-	-	+VE
C. albicans	17	15	14	12	10	-	-	-	+VE

Table 2. *Effect of catalyst on substitution of 2,6-dibromopyridine by various benzylamines.*

Entry	**Electrophilic Substrate**	**Nucleophilic Substrate**	**Yield (%)**
1	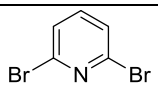	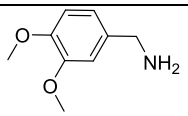	86
2	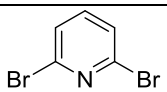	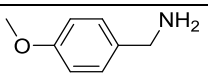	12
3	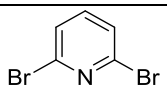	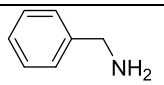	No reaction
4	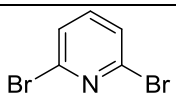	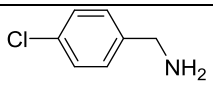	No reaction

3.5 Catalytic Activity of aah-CuNPs in the Synthesis of 6-bromo-N-(3,4-Dimethoxybenzyl)pyridin-2-amine

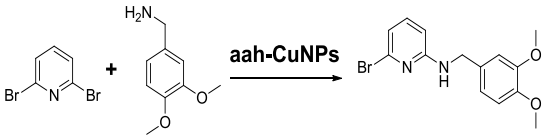

Scheme 1. aah-CuNPs *catalyzed Ullmannn amination reaction.*

The catalysis of Ullmann amination by aah-CuNPs was confirmed from ^{1}H NMR spectrum of the product formed. Figure 5 shows the ^{1}H-NMR spectrum of the product. The two high intensity singlets at 3.86 and 3.87 arise from the two methoxy groups. The pair of doublets at 4.40 and 4.38 and the triplet at 5.10 ppm are ascribed to the benzylic and NH protons, respectively, which confirm the substitution of dimethoxybenzylamine moiety. The remaining aromatic proton resonances correspond to the aryl and pyridine ring protons. Further, the ^{13}C NMR spectrum displays three aliphatic ^{13}C signals, besides 11 aromatic signals. Thus, the product formed contains a pyridine ring substituted with one benzylamine moiety. The complex pattern of splitting observed in the ^{1}H NMR spectrum did not permit complete elucidation of the structure of the product.

Therefore, HSQC and HMBC spectra of the product were recorded. All protons bonded directly to carbon atoms (C-H, one-bond coupling) were identified from the HSQC spectrum (see Figure 5a). Once C-H resonances were identified, three-bond C-H coupling data (Figure 5b) were used for assigning carbons without a hydrogen atom. This strategy helped in the identification of the carbons bearing the substitutions. Thus, the structure of 6-bromo-N-(3,4-dimethoxybenzyl)pyridin-2-amine was confirmed, which also helped in proving the catalytic activity of aah-CuNPs in nucleophilic substitution reaction. NMR Data (ppm): ^{1}H-NMR (400 MHz; $CDCl_3$): 3.86, s (3H), 3.87 s (3H), 4.39 d (2H), 5.10 t (NH), 6.27, d (1H), 6.74, d (1H), 6.82 d (1H), 6.865 md (1H), 6.89 md (1H), 7.21-7.27 q (1H); ^{13}C-NMR (100 MHz; $CDCl_3$): 158.73, 149.20, 148.40, 140.24, 139.58, 130.88, 119.65, 116.12, 111.22, 110.74, 104.72, 55.94, 55.90, 46.25.

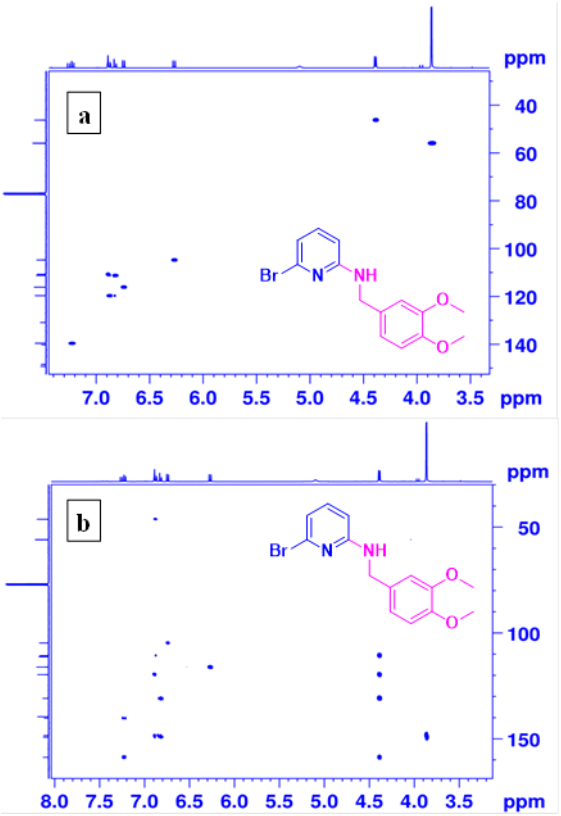

Figure 5. *$^{13}C–^{1}H$ HSQC (a) and $^{13}C–^{1}H$ HMBC (b) spectra of 6-bromo-N-(3,4-dimethoxybenzyl)pyridin-2-amine in $CDCl_3$.*

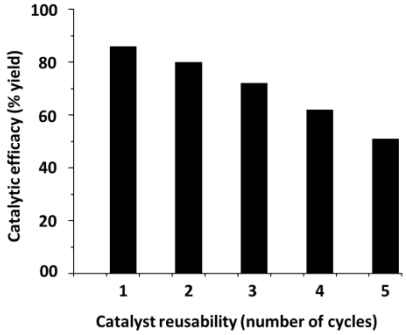

Figure 6. *Catalytic activity in consecutive cycles*

3.5 Reusability of Amido-Amino Clay Stabilized Copper Nanoparticles

After completion of Ullmann reaction, ethanol was added to the solution, and amido-amino halloysite stabilized copper nanoparticles were precipitated by centrifugation. The precipitate was washed with ethanol several times and isolated by centrifugation each time, and then it was reused in the Ullmann reaction involving 3,4-dimethoxybenzylamine.

Figure 6 shows the gradual degradation of the catalytic activity of aah-CuNPs during five consecutive cycles. After each catalytic cycle, the precipitated catalyst was transferred to the reaction vessel as a slurry in DMF and reused in subsequent cycles of Ullmann amination by 3,4-dimethoxybenazylamine.

4. CONCLUSION

In summary, a wet method for the preparation of amido-amino functional halloysite stabilized copper nanoparticles aah-CuNPs is described. Monodispersity and thermal stability of halloysite stabilized copper nanoparticles are confirmed. The functional groups that are responsible for the interaction between amido-amino halloysite and synthesized copper nanoparticles are identified. The concentration dependent antibacterial and antifungal efficacy of the synthesized aah-CuNPs is demonstrated. From this study, the minimum concentration required to demonstrate the zone of inhibition is deduced. Using high resolution NMR studies, the purity of the expected product and the reaction mechanism was studied. The catalytic activity of amido-amino halloysite supported copper nanoparticles is also demonstrated by attempting the nucleophilic substitution of 2,6-dibromopyridine by 3,4-dimethoxybenzy-lamine. In the absence of the catalyst, the above nucleophilic substitution reaction does not progress. Presence of aah-CuNPs (10%, w/w) promotes the reaction, which is completed in 4h at 110 °C. The protocol is simple and efficient, avoiding the need for inert atmosphere, additional base, or other additives. Only the mono-substituted product is formed in this Ullmann amination condition. This study offers a new method for the synthesis of mono substituted products from 2,6-dibromopyridine. Thus, the aah-CuNPs have the potential to be used as an antimicrobial agent and a reusable catalyst in Ullmann reaction.

ACKNOWLEDGEMENT

The authors wish to thank the Regional Research Institute of Unani Medicine, Royapuram, Chennai, for help in carrying out antimicrobial activity assay and the CATERS Research Facility, Central Leather Research Institute, Chennai, for NMR spectra.

REFERENCES

1. Liu, S., Pestano, J. P. C., Wolf, C., (2007). “Regioselective copper-catalyzed C-N and C-S bond formation using amines, thiols and halobenzoic acids”, *Synthesis,* 22: 3519-3527.
2. Ayoman , E., Hossini, G., N. Haghighi, N., (2015). “Synthesis of CuO nanoparticles and study on their catalytic properties”, *Int. J. Nanosci. Nanotechnol.,* 11: 63-70.
3. Rahimi, P., Hashemipour, H., Ehtesham Zadeh, M., Ghader, S., (2010). “Experimental investigation on the synthesis and size control of copper nanoparticle via chemical reduction method”, *Int. J. Nanosci. Nanotechnol*., 6: 144-149.
4. Shadrokh, Z., Yazdani, A., Eshghi, H., (2017). “Study on structural and optical properties of wurtzite Cu_2ZnSnS_4 nanocrystals synthesized*via* solvothermal method”, *Int. J. Nanosci. Nanotechnol*., 13: 359-366.
5. Ahmadi, R., Razaghian, A., Eivazi, Z., Shahidi, K., (2018). “Synthesis of Cu-CuO and Cu-Cu_2O nanoparticles via electro-explosion of wire method”, *Int. J. Nanosci. Nanotechnol*., 14: 93-99.
6. Khorshidi, A. R., Sh. Shariati, Sh., (2016). “-OSO_3H Functionalized mesoporous MCM-41 coated on Fe_3O_4 nanoparticles: an efficient and recyclable nano-catalyst for preparation of 3,2′-bisindoles”, *Int. J. Nanosci. Nanotechnol*., 12: 139-147.
7. Maleki, A., (2016). “Efficient synthesis of 2, 3-dihydroquinazolin-4(1H)-ones in the presence of ferrite/chitosan as a green and reusable nanocatalyst”, *Int. J. Nanosci. Nanotechnol*., 12: 215-222.

8. Keshipour, S., Kalam Khalteh, N., (2017). “Pd and Fe_3O_4 Nanoparticles supported on -٢)-N acetamide functionalized (aminoethylcellulose as an efficient catalyst for ,epoxidation of styrene”*Int. J. Nanosci. Nanotechnol*., 13: 219-226.
9. Anaraki Firooz, A., (2018). “Mo-Doped SnO_2 nanoparticles: a case study for selective epoxidation of cycloocten”, *Int. J. Nanosci. Nanotechnol*., 14: 159-163.
10. Crabbe, B. W., Kuehm, O. P., Bennettb, J. C., Hallett-Tapley, G. L., (2018). “Light-activated Ullmann homocoupling of aryl halides catalyzed using gold nanoparticle-functionalized potassium niobium oxides”, *Catal. Sci. Technol.*, 8: 4907-4915.
11. Kunz, K., Scholz, U., Ganzer, D., (2003). “Renaissance of Ullmann and Goldberg reactions - progress in copper catalyzed C-N-, C-O- and C-S-coupling”, *Synlett.*, 15: 2428-2439.
12. Shaughnessy, K. H., Ciganek, E., DeVasher, R. B., (2014). “Copper-catalysed amination of aryl and alkenyl electrophiles”, *Org. React*. 85: 1-668.
13. Hartwig, J. F., (2008). “Evolution of a fourth generation catalyst for the amination and thioetherification of aryl halides”, *Acc. Chem. Res*. 41: 1534-1544.
14. M. Cortes-Salva, M., Garvin, C., Antilla, J. C., (2011). “Ligand-free copper-catalyzed arylation of amidines”, *J. Org. Chem*., 76: 1456-1459.
15. Yang, X., Liu, H., Fu, H., Qiao, R., Jiang, Y., Zhao, Y., (2010). “Efficient Copper-Catalyzed Synthesis of 4-Aminoquinazoline and 2,4-Diaminoquinazoline Derivatives”, *SynLett.*, 1: 101-106.
16. Wolf, C., Liu, S., Mei, X., August, A. T., Casimir, M. D., (2006). “Regioselective Copper-Catalyzed Amination of Bromobenzoic Acids Using Aliphatic and Aromatic Amines”, *J. Org. Chem*., 71: 3270-3273.
17. Kwong, F. Y., Klapars, A., Buchwald, S. L., (2002). “Copper-catalyzed coupling of alkylamines and aryl iodides: an efficient system even in an air atmosphere”, *Org. Lett*., 4: 581-584.
18. Jiao, J., Zhang, X.-R., Chang, N.-H., Wang, J., Wei, J.-F., Shi, X.-Y., Chen, Z.-G., (2011). “A facile and practical copper powder-catalyzed, organic solvent- and ligand-free Ullmann amination of aryl halides”, *J. Org. Chem*., 76: 1180-1183.
19. Zhang, Y., Yang, X., Yao, Q., Ma, D., (2012). “CuI/DMPAO-Catalyzed N-Arylation of Acyclic Secondary Amines”, *Org. Lett*., 14: 3056-3059.
20. Zhou, W., Fan, M., Yin, J., Jiang, Y., Ma, D., (2015). “CuI/Oxalic diamide catalyzed coupling reaction of (hetero)aryl chlorides and amines”, *J. Am. Chem. Soc*., 137: 11942-11945.
21. Gao, J., Bhunia, S., Wang, K., Gan, L., Xia, S., Ma, D., (2017). “Discovery of N-(Naphthalen-1-yl)-N′-alkyl Oxalamide Ligands Enables Cu-Catalyzed Aryl Amination with High Turnovers”, *Org. Lett*., 19: 2809-2812.
22. Chen, Y.-J., Chen, H.-H., (2006). “1,1,1-Tris(hydroxymethyl)ethane as a new, efficient, and versatile tripod ligand for copper-catalyzed cross-coupling reactions of aryl iodides with amides, thiols, and phenols”, *Org. Lett*., 8: 5609-5612.
23. Vandarkuzhali, S. A. A., Radha, N., Pandian, K., (2013). “Water Soluble Iron aminoclay for Catalytic Reduction of Nitrophenol”, *Orient. J. Chem*., 29: 661-665.
24. Ramya, R., Jaculin Raiza, A., Devi, S., Raghunathan, R., Pandian, K., (2014-2015). “Synthesis of aminoclay protected palladium nanoparticles and study its catalytic activity in organic synthesis”, *Int. J. ChemTech Res*., 7: 1297-1302.
25. Datta, K. K. R., Kulkarni, C., Eswaramoorthy, M., (2012). “Aminoclay: a permselective matrix to stabilize copper nanoparticles”, Chem. Commun., 46: 616-618.
26. Raji, M., Mekhzoum, M. E. M., el Kacem Qaiss, A., Bouhfid, R., (2016). “*Nanoclay modification and functionalization for nanocomposites development: Effect on the structural, morphological, mechanical and rheological properties. In Nanoclay Reinforced Polymer Composites*”, Springer, Berlin, Germany.
27. Luty´nski, M., Sakiewicz, P., Luty´nska, S., (2019). “Characterization of diatomaceous earth and halloysite resources of Poland”, *Minerals*, 9: 670; doi:10.3390/min9110670.
28. Zhang, P., Shao, C., Zhang, Z., Zhang, M., Mu, J., Guo, Z., Liu, Y., (2011). “In situ assembly of well-dispersed Ag nanoparticles (AgNPs) on electrospun carbon nanofibers (CNFs) for catalytic reduction of 4-nitrophenol”, *Nanoscale*, 3: 3357-3363.
29. Pinto, R. J. B., Neves, M. C., Neto, C. P., Trindade, T., (2013). “*Composites of cellulose and metal nanoparticles: In Nanocomposites – New trends and developments*”, Ebrahimi F., Ed., 2012, 73-96.
30. Liu, S., Hu, M., Zeng, T. H., Wu, R., Jiang, R., Wei, J., Wang, L., Kong, J., Chen, Y., (2012). “Lateral dimension-dependent antibacterial activity of graphene oxide sheets”, *Langmuir*, 28: 12364-12372.